

^{75}As NMR local probe study of magnetism in $(\text{Eu}_{1-x}\text{K}_x)\text{Fe}_2\text{As}_2$

Tusharkanti Dey,^{1,*} P. Khuntia,^{1,†} A.V. Mahajan,¹ Anupam,² and Z. Hossain²

¹*Department of Physics, Indian Institute of Technology Bombay, Powai, Mumbai 400076, India*

²*Department of Physics, Indian Institute of Technology Kanpur, Kanpur 208016, India*

Abstract

^{75}As NMR measurements were performed as a function of temperature and doping in $\text{Eu}_{1-x}\text{K}_x\text{Fe}_2\text{As}_2$ ($x = 0.5, 0.7$) samples. The large Eu^{2+} moments and their fluctuations are found to dominate the ^{75}As NMR properties. The ^{75}As nuclei close to the Eu^{2+} moments likely have a very short spin-spin relaxation time (T_2) and are wiped out of our measurement window. The ^{75}As nuclei relatively far from Eu^{2+} moments are probed in this study. Increasing the Eu content progressively decreases the signal intensity with no signal found for the full-Eu sample ($x = 0$). The large ^{75}As NMR linewidth arises from an inhomogeneous magnetic environment around them. The spin lattice relaxation rate ($1/T_1$) for $x = 0.5$ and 0.7 samples is nearly independent of temperature above 100 K and results from a dipolar coupling to paramagnetic fluctuations of the Eu^{2+} moments. The behavior of $1/T_1$ at lower temperatures has contributions from the antiferromagnetic fluctuations of the Eu^{2+} moments as also the fluctuations intrinsic to the FeAs planes and from superconductivity.

PACS numbers: 74.70.Xa, 74.25.nj, 74.62.Dh

I. INTRODUCTION

The interest in high temperature superconductivity experienced a resurgence after the discovery of superconductivity in $\text{LaFeAs}(\text{O}_{1-x}\text{F}_x)$ with a superconducting transition temperature $T_c = 26$ K [1]. So far, hundreds of materials in the iron pnictide family have been found to be superconducting [2, 3], some with transition temperatures ranging upto 56 K [4]. These materials broadly belong to 4 groups based on their crystal structure. The quaternary ‘1111’ compounds with chemical formula RFeAsO where R is a rare earth element [1, 5], ternary arsenides (‘122’) AFe_2As_2 with $\text{A} = \text{Ba}, \text{Sr}, \text{Ca}$ and Eu [6–9], ‘111’ compounds $(\text{Li}/\text{Na})\text{FeAs}$ [10, 11] and the ‘11’ binary chalcogenides FeSe_{1-x} [12]. Among them, ‘122’ series materials are studied most because of their rich phase diagram although the highest T_C obtained is relatively lower than for ‘1111’ series materials.

Like other parent compounds in the ‘122’ series iron arsenide family, EuFe_2As_2 crystallizes in ThCr_2Si_2 -type structure ($I4/mmm$) and undergoes a spin density wave (SDW) transition related to the Fe moments at ~ 200 K, confirmed by heat capacity and resistivity measurements [13, 14]. But EuFe_2As_2 is a very special member in the ‘122’ family as it contains two different magnetic atoms. It is the only known member of the ‘122’ family which contains $4f$ electrons. The Eu^{2+} ions have a large magnetic moment of $7\mu_B$ and they order ferromagnetically within the ab plane and antiferromagnetically with neighboring planes along the c -axis at 20 K [13, 14]. Besides multiple magnetic transitions, appearance of superconductivity is reported in EuFe_2As_2 by hole/electron/isovalent doping [9, 15, 16], and also by

applying external pressure [17]. It is also reported that magnetic ordering of Eu^{2+} moments and superconductivity coexist in this system at low temperature [15, 18]. This material is a good candidate to study the interplay between superconductivity and Eu^{2+} moments ordering.

Jeevan *et al.* [9] first reported that 50% K substitution in EuFe_2As_2 system suppresses the SDW transition and in turn gives rise to high-temperature superconductivity below 32 K. They also found a signature of Eu^{2+} magnetic ordering from their specific heat data. From ^{57}Fe and ^{151}Eu Mossbauer spectroscopic study on $\text{Eu}_{0.5}\text{K}_{0.5}\text{Fe}_2\text{As}_2$, Anupam *et al.* [18] found no signature of a SDW transition but Eu^{2+} ordering is found at 10 K. Subsequently, they constructed the phase diagram of the $\text{Eu}_{1-x}\text{K}_x\text{Fe}_2\text{As}_2$ ($0 \leq x \leq 1$) system [19]. The SDW transition corresponding to the Fe-sublattice coexists with superconductivity with a lower $T_C = 5.5$ K in the underdoped sample ($x = 0.15$). As the doping percentage increases ($x = 0.3$) the SDW transition vanishes and superconductivity appears at relatively higher $T_C = 20$ K. The maximum $T_C = 32$ K is obtained for $x = 0.5$. Coexistence of Eu^{2+} magnetic ordering with superconductivity is sustained upto $x = 0.6$.

Iron arsenide superconductors have been extensively studied using NMR to obtain a deeper understanding of various physics issues [20–24]. In this $\text{Eu}_{1-x}\text{K}_x\text{Fe}_2\text{As}_2$ system also ^{75}As NMR measurements could be a useful probe to understand the interplay of magnetic ordering and superconductivity. Till date only two publications on NMR in EuFe_2As_2 and related systems have been reported [25, 26]. In the former, ^{75}As NMR measurements are reported on single-crystal of $\text{EuFe}_{1.9}\text{Co}_{0.1}\text{As}_2$ which does not show superconductivity but undergoes an SDW transition at 120 K [25]. The latter reports ^{75}As NMR measurements on a $\text{Eu}_{0.2}\text{Sr}_{0.8}(\text{Fe}_{0.86}\text{Co}_{0.14})_2\text{As}_2$ single crystal, which shows a superconducting transition below 20 K [26]. However no NMR study has been reported on the $\text{Eu}_{1-x}\text{K}_x\text{Fe}_2\text{As}_2$ series which could be useful to understand how the presence of Eu^{2+} moments affects the magnetic properties of the material. We have performed

*Email: tusdey@gmail.com; Present address: IFW Dresden, 01171 Dresden, Germany

†Present address: Max-Planck Institute for Chemical Physics of Solids, D-01187 Dresden, Germany

a ^{75}As NMR study on different doping concentrations ($x = 0, 0.38, 0.5, 0.7$) in $(\text{Eu}_{1-x}\text{K}_x)\text{Fe}_2\text{As}_2$ to understand the evolution of NMR parameters with doping and temperature. Our bulk measurements show appearance of superconductivity for the $x = 0.38, 0.5$ and 0.7 samples with highest $T_C = 32\text{K}$ for the $x = 0.5$ sample. For the $x = 0$ sample, no superconductivity is found but the SDW transition is present at 197K . However, the SDW transition is suppressed for the other three samples ($x = 0.38, 0.5, 0.7$). The ordering of the Eu^{2+} moments is observed at 20K , 10K and 7K for the $x = 0, 0.38$ and 0.5 samples, respectively but no ordering of the Eu^{2+} moments is found for $x = 0.7$. The magnetic properties of the samples are dominated by the large moment of Eu^{2+} ions. The ^{75}As nuclei close to the Eu^{2+} moments have a very short spin-spin relaxation time (T_2) driving them out of the measurement window. This results in a drop in the integrated signal intensity with increasing Eu-content and no signal was observed with our measurement conditions for the full Eu ($x = 0$) sample. Presence of unequal environments for the ^{75}As nuclei (some near Eu moments and some not) gives rise to broad and asymmetric spectra. The temperature dependence of the ^{75}As NMR shift (as determined from the centre-of-gravity) has a Curie-Weiss behavior reflecting the paramagnetism of the Eu^{2+} spins. From our measurements ($x = 0.5, 0.7$), we find that the $1/T_1$ is nearly temperature independent above 100K (and much enhanced compared to analogous compositions not containing Eu). This is due to the paramagnetic fluctuations of the Eu^{2+} moments. The T -dependence at lower temperatures may be related to the intrinsic behavior of the FeAs planes.

II. EXPERIMENTAL DETAILS

Polycrystalline samples of $\text{Eu}_{1-x}\text{K}_x\text{Fe}_2\text{As}_2$ ($x = 0, 0.38, 0.5, 0.7$) were prepared by solid state reaction methods as detailed in Ref. [19].

We have performed ^{75}As NMR measurements on $(\text{Eu}_{1-x}\text{K}_x)\text{Fe}_2\text{As}_2$ ($x = 0, 0.38, 0.5, 0.7$) samples using a Tecmag pulse spectrometer in a magnetic field of 93.954kOe obtained inside a room-temperature bore Varian superconducting magnet. For variable temperature measurements, we have used an Oxford continuous flow cryostat. Liquid nitrogen and liquid helium were used as coolants in the temperature range $80\text{--}300\text{K}$ and $4\text{--}80\text{K}$, respectively. For NMR measurements, we tried to align the powder samples by mixing with Stycast 1266 epoxy and then curing overnight in an external magnetic field $H = 93.954\text{kOe}$. Our measurements indicate that although the spectral width is reduced significantly, the samples are not oriented fully. The ^{75}As has a nuclear spin $I = 3/2$ (100% natural abundance) with gyromagnetic ratio $\gamma/2\pi = 7.2919\text{MHz/T}$. Frequency sweep spectra at a few temperatures were constructed by plotting the integral of the spin echo (resulting from a $\pi/2 - \tau - \pi/2$ pulse sequence with $\tau \geq 35\mu\text{s}$) at different transmitter

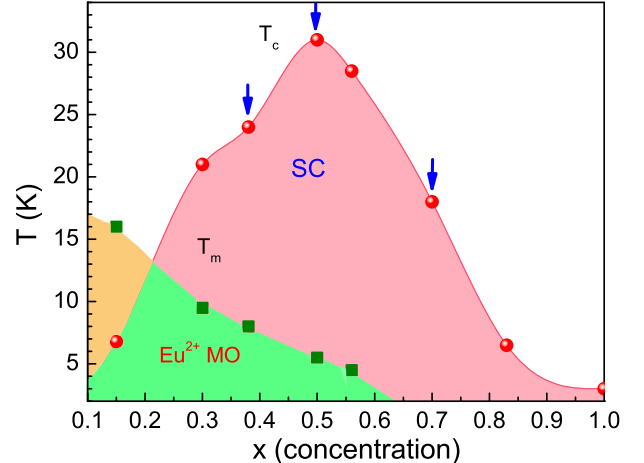


Figure 1: The phase diagram of $(\text{Eu}_{1-x}\text{K}_x)\text{Fe}_2\text{As}_2$ samples showing the superconducting transition temperature (T_C) and Eu^{2+} magnetic ordering temperature (T_m) as a function of K content x . The figure is adapted from Ref. [19]. The compositions used in the present work are indicated with arrows.

frequencies. Spin-lattice relaxation was measured using the saturation recovery method.

III. RESULTS AND DISCUSSIONS

Phase purity of the samples was confirmed by powder x-ray diffraction (XRD) measurements. Detailed analysis of the XRD data (reported in Ref. [19]) shows that lattice parameter a decreases while c and the unit cell volume increase with increasing doping percentage x .

Magnetic susceptibility and resistivity of the samples were measured as a function of temperature and are reported in Ref. [19]. A phase diagram showing the Eu^{2+} moments ordering and the superconducting transition temperature as a function of doping percentage is shown in Fig. 1. This phase diagram is adapted from Ref. [19] based on measurements on the same samples as used in the current study. Four of these samples ($x = 0, 0.38, 0.5, 0.7$) are studied in this present work.

Following these basic characterizations, we investigated the normal state properties using ^{75}As NMR as a local probe. Since the ^{75}As nucleus ($I = 3/2$) is not at a site of cubic symmetry, a non-zero electric field gradient (EFG) will be present at the ^{75}As site. The interplay between this EFG and the quadrupole moment of ^{75}As nucleus will create one central line ($-1/2 \rightarrow 1/2$ transition) along with satellite peaks ($-3/2 \rightarrow -1/2$ and $3/2 \rightarrow 1/2$ transitions) on either side of the central line in the spectra. A powder pattern is expected for randomly oriented polycrystalline samples. In the present case, we could obtain a partial alignment with a significant reduction

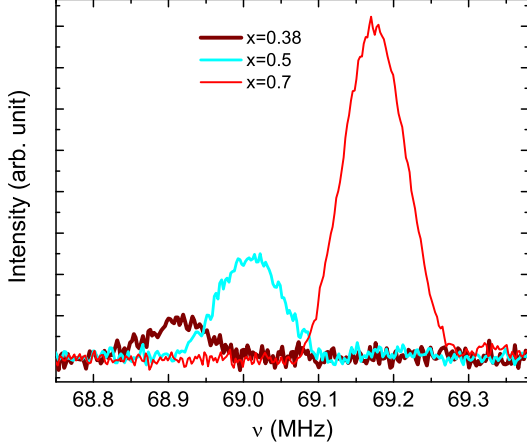


Figure 2: Fourier transform of the spin echo for different compositions at room temperature. The transmitter frequency was adjusted to the position of the peak in each case. Other than that, these measurements are done with identical conditions (coil, filling factor, etc.) and the intensities are normalized to the number of ^{75}As nuclei present (depends on the molecular weight of a composition and the mass taken) in the sample.

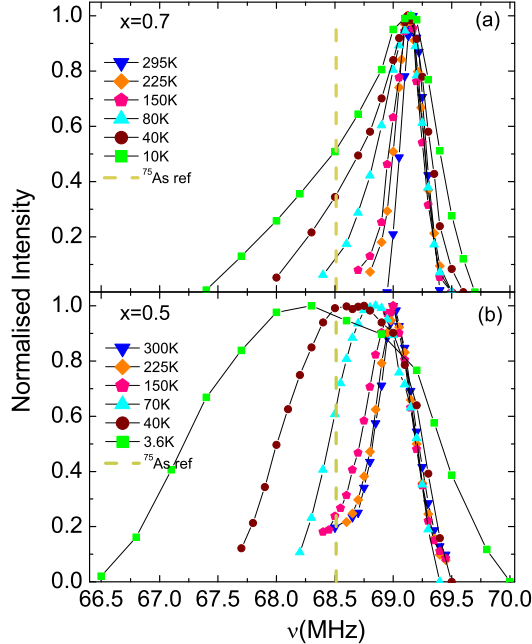


Figure 3: ^{75}As NMR spectra of $x = 0.5$ and 0.7 samples measured at different temperatures obtained from an integral of the echo at different frequencies. The ^{75}As reference line is shown as dashed line.

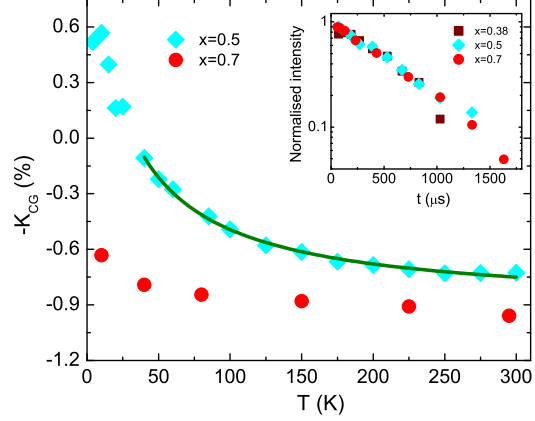


Figure 4: ^{75}As NMR shift (determined using the cg) is shown as a function of temperature for the $x = 0.5$ and 0.7 samples. The green solid line is a fit to CW law. Inset: Spin-spin relaxation (T_2) decay curves for $x = 0.38, 0.5$ and 0.7 samples measured at room temperature.

in the width of the central line. We report our measurements on the central line of these partially aligned samples. We have noticed that as the doping percentage x decreases, the signal intensity gets reduced and no signal is found for the $x = 0$ sample. To quantify this issue, we have measured the spin-echo for different compositions at their respective spectral peak positions under identical measurement parameters. The Fourier transforms of the spin-echos after normalizing to the number of ^{75}As nuclei present in the sample are shown in Fig. 2. It is clearly seen that the signal intensity sharply falls with decreasing x i.e increasing Eu content. The ratio of the integrated intensity at room temperature (spectral width is taken into account) for $x = 0.7$ and 0.5 samples is roughly $1 : 0.5$. Figure 2 suggests that the integrated intensity for the $x = 0.38$ sample would be much lower than the other two samples.

In $(\text{Eu}_{1-x}\text{K}_x)\text{Fe}_2\text{As}_2$ samples, the $2a$ site is occupied by Eu^{2+} and K^+ ions. In general, the two types of ions occupy the sites statistically. While the Eu^{2+} has a large moment, K^+ does not carry a moment. There will be a fraction of ^{75}As nuclei which are close to the Eu^{2+} moments while some others will be far from Eu^{2+} moments along with all intermediate possibilities. The ^{75}As nuclei situated in close proximity to the Eu^{2+} moments are likely to have a very short spin-spin relaxation time T_2 as also a short spin-lattice relaxation time T_1 . Guguchia *et al.* [25] measured ^{75}As T_2 for $\text{EuFe}_{1.9}\text{Co}_{0.1}\text{As}_2$ as a function of temperature. The T_2 at room temperature was found to be $\sim 32\mu\text{s}$ and further decreases with decreasing temperature giving rise to a wipeout effect with nearly 90% of the signal lost by 100 K. A similar situation is expected for our $x = 0$ sample since the composition is nearly the same. Further, in our measurements the time

delay between the echo forming pulses is larger than $35\mu\text{s}$ which leads to a significant wipeout even at room temperature. Even in our other compositions, the ^{75}As nuclei close to Eu^{2+} moments are expected to have a short T_2 and are wiped out of our measurement window. Consequently, our measurements pertain to nuclei which are relatively far from Eu^{2+} moments. This fraction is seen to grow with decreasing europium content. That we are measuring only nuclei which are far from Eu^{2+} moments is evident from our T_2 measurements (shown in the inset of Fig. 4). For all the three samples ($x = 0.38, 0.5, 0.7$) T_2 at room temperature is $\sim 600\mu\text{s}$. Because of a very low signal intensity for the $x = 0.38$ sample, we have performed temperature dependent study on $x = 0.5$ and 0.7 samples only.

A wide distribution of magnetic environments at the ^{75}As sites gives rise to very broad spectra as shown in Fig. 3. This distribution is greater for the $x = 0.5$ composition than the $x = 0.7$ composition, as might be expected. The central line of the spectra at different temperatures are constructed by plotting the spin-echo intensity as a function of measuring frequency. Evolution of the spectra with temperature are shown in Fig. 3(b) and Fig. 3(a) for $x = 0.5$ and $x = 0.7$ samples, respectively.

Spectra at room temperature for all the three samples are shifted positively from the reference frequency. The shift at room temperature is dependent on the Eu-content and varies linearly with x . Spectra for the $x = 0.5$ sample (Fig. 3(b)) are almost symmetric at all temperatures in contrast to that for the $x = 0.7$ sample. A possible explanation is that in this case, there is an equal distribution of ^{75}As nuclei with more or less Eu neighbours (assuming statistical occupancy of Eu and K). Further we have studied the variation of ^{75}As NMR spectra and shift with temperature. We have considered the centre of gravity (cg) of the spectra to calculate the shift (K_{cg}). The temperature dependence of shift is plotted in Fig. 4. Although the shift is positive at room temperature, it decreases with decreasing temperature and becomes negative at low temperature. This temperature variation of K_{cg} follows the CW law [$K_{cg}(T) = K_0 + C/(T - \theta)$] in the temperature range $40 - 300\text{K}$ and yields $K_0 = 0.91\%$ and $\theta = -24\text{K}$ (see Fig. 4). The T -independent part K_0 could be partly arising from the orbital shift while a part of it can also be due to the intrinsic susceptibility of the FeAs planes.

On the other hand, for the $x = 0.7$ sample has a weaker temperature dependence of K_{cg} (Fig. 4). The spectrum is symmetric at room temperature but becomes asymmetric at lower temperatures (Fig. 3(a)). In this sample, since K percentage is much more than Eu, there will be a large fraction of ^{75}As nuclei far from Eu^{2+} moments. Their resonance frequency does not shift much with temperature while the ones near Eu moments shift in a CW manner with decreasing temperature which explains the increasing asymmetry at lower temperatures. Finally, the magnetic properties of the samples are dominated by the Eu^{2+} moments and the ^{75}As nuclei have a negative

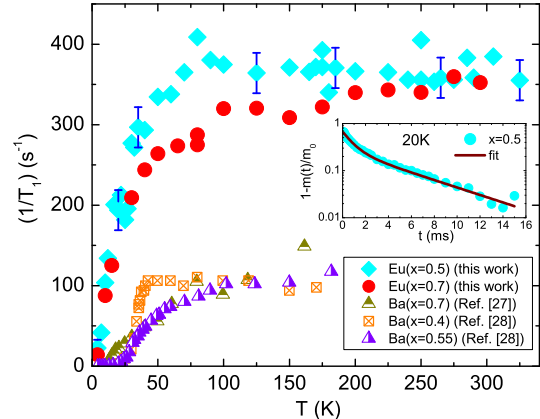


Figure 5: Spin-lattice relaxation rate ($1/T_1$) for $x = 0.5$ and $x = 0.7$ samples are shown as a function of temperature. Relaxation rate for $\text{Ba}_{0.3}\text{K}_{0.7}\text{Fe}_2\text{As}_2$ [$\text{Ba}(x = 0.7)$] taken from Ref. [27] and for $\text{Ba}_{0.6}\text{K}_{0.4}\text{Fe}_2\text{As}_2$ [$\text{Ba}(x = 0.4)$] and $\text{Ba}_{0.45}\text{K}_{0.55}\text{Fe}_2\text{As}_2$ [$\text{Ba}(x = 0.55)$] taken from Ref. [28] are also shown for comparison. Inset: A representative spin-lattice relaxation recovery curve for the $x = 0.5$ sample measured at 20K is shown.

hyperfine coupling with the Eu^{2+} moments, similar as found in Ref. [25].

To study the low energy spin dynamics, we have measured the spin-lattice relaxation rate ($1/T_1$) as a function of temperature by the saturation recovery method for both the samples ($x = 0.5, 0.7$). Since the spectra are very broad, it was difficult to saturate the full central line with a single pulse. For the $x = 0.5$ sample, we have used a comb of saturating pulses with total duration much greater than T_1 in the pulse sequence ($n \times \pi/2 \dots t \dots \pi/2 \dots \pi$) to saturate the central line. On the other hand, for the $x = 0.7$ sample the duration of saturating pulses used is much less than T_1 since the spectral width is relatively less. Consequently, the time dependence of the recovery of longitudinal magnetization $m(t)$ is fitted with Eq. 1 (for the $x = 0.5$ sample) and with Eq. 2 (for the $x = 0.7$ sample) to extract T_1 at individual temperatures.

$$1-m(t)/m_0 = A(0.4 \exp(-t/T_1) + 0.6 \exp(-6t/T_1)) \quad (1)$$

$$1-m(t)/m_0 = A(0.1 \exp(-t/T_1) + 0.9 \exp(-6t/T_1)) \quad (2)$$

The former equation is valid for $I = 3/2$ nuclei when only the central line is saturated with a saturation sequence with duration much greater than T_1 [30]. The latter is valid when the saturating comb has a duration much less than T_1 [31, 32]. The coefficient A takes into account the deviation from complete saturation.

A representative longitudinal nuclear magnetization recovery curve for $x = 0.5$ sample is shown in the inset of Fig. 5 along with its fit with Eq. 1. The relaxation

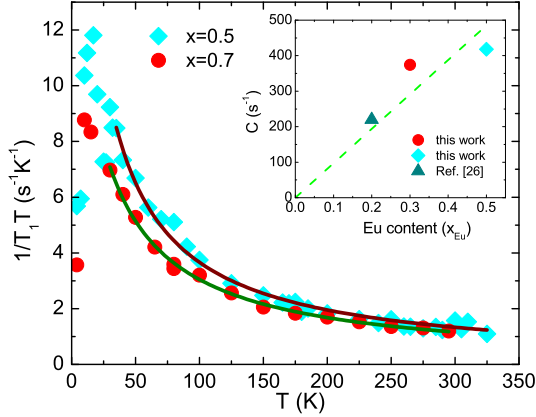


Figure 6: $1/T_1T$ is shown as a function of temperature. The solid lines are Curie–Weiss fits (described in the text). Inset: Curie constant C plotted as a function of Eu content x_{Eu} . The data point for $x_{\text{Eu}} = 0.2$ is for $\text{Eu}_{0.2}\text{Sr}_{0.8}(\text{Fe}_{0.86}\text{Co}_{0.14})_2\text{As}_2$ taken from Ref. [26]. The dashed line is a guide to eye.

rates ($1/T_1$) for both the samples are plotted as a function of temperature in Fig. 5. We have also shown the relaxation rate ($1/T_1$) of $\text{Ba}_{0.3}\text{K}_{0.7}\text{Fe}_2\text{As}_2$ measured with $H \parallel ab$ taken from Ref. [27] and of $\text{Ba}_{0.6}\text{K}_{0.4}\text{Fe}_2\text{As}_2$ and $\text{Ba}_{0.45}\text{K}_{0.55}\text{Fe}_2\text{As}_2$ taken from Ref. [28]. These materials can be considered as Ba (non magnetic) analogs of our Eu-based samples. The relaxation rates of our Eu-based samples are more than two times larger than those of the Ba based samples. It seems evident that the higher relaxation rate arises from a coupling to the fluctuating Eu^{2+} moments in our samples. Due to the same reason the rate is higher for the $x = 0.5$ sample which contains more Eu than the $x = 0.7$ sample. There is no signature of SDW transition or Eu^{2+} moments ordering in our T_1 measurements. For both the samples $1/T_1$ is almost independent of temperature at high temperature but drops at low temperature indicating the superconducting transition taking place in these samples. The superconducting gap slows down the relaxation process while the Eu^{2+} moments fluctuations tries to increase the rate. Probably the interplay of these two makes a broad transition. Similar behavior is also reported in case of $\text{Eu}_{0.2}\text{Sr}_{0.8}(\text{Fe}_{0.86}\text{Co}_{0.14})_2\text{As}_2$ [26].

In Fig. 6, we have plotted $1/T_1T$ as a function of temperature and fitted with the CW law ($\frac{1}{T_1T} = \frac{C}{(T-\theta)}$) in the temperature range ≥ 30 K (shown as solid lines). The fitting yields $C = 374\text{s}^{-1}$ and $\theta = -22\text{K}$ for $x = 0.7$ sample and $C = 418\text{s}^{-1}$ and $\theta = -14\text{K}$ for the $x = 0.5$ sample. It has been claimed that the Curie–Weiss behavior of $1/T_1T$ indicates that the spin-lattice relaxation process is dominated by 2D antiferromagnetic spin fluctuations [26]. However it is apparent that the relaxation here is driven by fluctuations of the Eu^{2+} moments (which are three dimensional) and have little to do with

the dynamical susceptibility of the FeAs planes. In fact, we see from the inset of Fig. 6 that the Curie constant in $1/T_1T$ decreases linearly with decreasing Eu content and extrapolates to zero for $x = 0$. In reality, the $1/T_1$ of $\text{Ba}_{0.3}\text{K}_{0.7}\text{Fe}_2\text{As}_2$ (Eu-free analog) appears to vary almost linearly with T [27] which means that $1/T_1T$ will be nearly T -independent. This further supports the fact that the relaxation process in our samples is dominated by the Eu^{2+} moments fluctuations. Indeed, the spin-lattice relaxation rate is given by [29]

$$1/T_1 = \frac{2k_B T}{N_A \hbar^2} \left(\frac{\gamma_n}{\gamma_e} \right)^2 A_{hf}^2 \Sigma \frac{\chi''(q, \omega)}{\omega} \quad (3)$$

where A_{hf} is the hyperfine coupling constant, $\chi''(q, \omega)$ is the imaginary part of the dynamical susceptibility per mole of electronic spin at the Larmor frequency ω , k_B is the Boltzmann constant, γ_n and γ_e are nuclear and electronic gyromagnetic ratios, respectively. The summation reduces to $\frac{\chi(T)\tau}{2\pi}$ where $\chi(T)$ is the static susceptibility of the impurity moments. If the relaxation of the impurity Eu^{2+} spins is dominated by the interaction among them, then $1/\tau = \omega/2\pi$ (with $\omega^2 = 8J_{int}^2 z S(S+1)/3\hbar^2$, where z is the number of nearest neighbors with interaction J_{int}) is temperature independent. This quite naturally leads to $1/T_1T \propto \chi(T)$ as is observed. Quantitatively speaking, we calculated J_{int} considering $\theta = 2zS(S+1)/3k_B$ (taken to be 20K) where the number of near neighbours for each Eu ($S = 1/2$) is $z = 6$. This yields $\omega \approx 4.8 \times 10^{11}$ rad/s. The dipolar field A_{dip} was calculated [29] at the As site from Eu spins by computing $7[\sqrt{2\pi}g^2\mu_B^2 \Sigma 1/r_i^6]^{1/2}$. Here r_i is the distance of the i^{th} Eu atom from a given As nucleus and the sum is over the Eu neighbours of an As nucleus. The summation converged beyond 100 unit cells and yielded $A_{dip} = 3.65$ kOe. Taking the susceptibility of EuFe_2As_2 as [14] $\chi = 7.58/(T+20)$ cm^3/mole , the room temperature value of $1/T_1T$ was obtained to be about $18\text{s}^{-1}\text{K}^{-1}$. The observed value of about 1 at room temperature is then reasonable considering the smaller concentration of Eu in $x = 0.5$ or 0.7 . The contribution due to the hyperfine coupling to the Eu spins is expected to be an order of magnitude smaller than the observed value.

IV. CONCLUSIONS

We have performed ^{75}As NMR measurements on $(\text{Eu}_{1-x}\text{K}_x)\text{Fe}_2\text{As}_2$ ($x = 0.38, 0.5, 0.7$) samples. Our bulk measurements show no superconductivity but a SDW transition at 197K for the $x = 0$ sample. This SDW transition is suppressed and superconductivity appears for the $x = 0.38, 0.5$ and 0.7 samples. The properties of the samples are largely dominated by the Eu^{2+} moments. The ^{75}As nuclei close to the Eu^{2+} moments have a very short T_2 and are driven out of our measurement window. This results in a sharp drop of signal intensity with increasing Eu-content in the sample and no signal is found

for the full Eu sample ($x = 0$). The temperature variation of the NMR shift and the spectra can be understood by considering a distribution of magnetic environments for the ^{75}As nuclei; some near Eu^{2+} local moments and some far away from them. The ^{75}As spin lattice relaxation rate ($1/T_1$) is seen to be dominated by the dipolar coupling to the Eu^{2+} moment fluctuations and the effect of the FeAs planes is seen only at lower temperatures

upon the onset of the superconducting transition.

V. ACKNOWLEDGMENT

We thank the Department of Science and Technology, Government of India for financial support.

-
- [1] Y. Kamihara, T. Watanabe, M. Hirano, and H. Hosono, *J. Am. Chem. Soc.* **130**, 3296 (2008).
- [2] D. C. Johnston, *Adv. Phys.* **59**, 803 (2010).
- [3] G. R. Stewart, *Rev. Mod. Phys.* **83**, 1589 (2011).
- [4] G. Wu, Y. L. Xie, H. Chen, M. Zhong, R. H. Liu, B. C. Shi, Q. J. Li, X. F. Wang, T. Wu, Y. J. Yan, J. J. Ying, and X. H. Chen, *J. Phys.: Condens. Matter* **21**, 142203 (2009).
- [5] X.H. Chen, T. Wu, G. Wu, R.H. Liu, H. Chen, and D.F. Fang, *Nature (London)* **453**, 761 (2008).
- [6] M. Rotter, M. Tegel, and D. Johrendt, *Phys. Rev. Lett.* **101**, 107006 (2008).
- [7] N. Ni, S. Nandi, A. Kreyssig, A. I. Goldman, E. D. Mun, S. L. Bud'ko, and P. C. Canfield, *Phys. Rev. B* **78**, 014523 (2008).
- [8] C. Krellner, N. Caroca-Canales, A. Jesche, H. Rosner, A. Ormeci, and C. Geibel, *Phys. Rev. B* **78**, 100504(R) (2008).
- [9] H. S. Jeevan, Z. Hossain, D. Kasinathan, H. Rosner, C. Geibel, and P. Gegenwart, *Phys. Rev. B* **78**, 092406 (2008).
- [10] J. H. Tapp, Z. Tang, B. Lv, K. Sasmal, B. Lorenz, P. C. W. Chu, and A. M. Guloy, *Phys. Rev. B* **78**, 060505(R) (2008).
- [11] D. R. Parker, M. J. Pitcher, P. J. Baker, I. Franke, T. Lancaster, S. J. Blundell, and S. J. Clarke, *Chem. Commun.* 2189 (2009).
- [12] F.-C. Hsu, J.-Y. Luo, K.-W. Yeh, T.-K. Chen, T.-W. Huang, P. M. Wu, Y.-C. Lee, Y.-L. Huang, Y.-Y. Chu, D.-C. Yan, and M.-K. Wu, *Proc. Natl. Acad. Sci. U.S.A.* **105**, 14262 (2008).
- [13] H. S. Jeevan, Z. Hossain, D. Kasinathan, H. Rosner, C. Geibel, and P. Gegenwart, *Phys. Rev. B* **78**, 052502 (2008).
- [14] Z. Ren, Z. Zhu, S. Jiang, X. Xu, Q. Tao, C. Wang, C. Feng, G. Cao, and Z. Xu, *Phys. Rev. B* **78**, 052501 (2008).
- [15] Z. Ren, Q. Tao, S. A. Jiang, C. M. Feng, C. Wang, J. H. Dai, G. H. Cao, and Z. A. Xu, *Phys. Rev. Lett.* **102**, 137002 (2009).
- [16] S. Jiang, H. Xing, G. Xuan, Z. Ren, C. Wang, Z. Xu, and G. Cao, *Phys. Rev. B* **80**, 184514 (2009).
- [17] C. F. Miclea, M. Nicklas, H. S. Jeevan, D. Kasinathan, Z. Hossain, H. Rosner, P. Gegenwart, C. Geibel, and F. Steglich, *Phys. Rev. B* **79**, 212509 (2009).
- [18] Anupam, P. L. Paulose, H. S. Jeevan, C. Geibel, and Z. Hossain, *J. Phys.: Condens. Matter* **21**, 265701 (2009).
- [19] Anupam, P. L. Paulose, S. Ramakrishnan, and Z. Hossain, *J. Phys.: Condens. Matter* **23**, 455702 (2011).
- [20] K. Ishida, Y. Nakai, and H. Hosono, *J. Phys. Soc. Jpn.* **78**, 062001 (2009).
- [21] Y. Nakai, T. Iye, S. Kitagawa, K. Ishida, S. Kasahara, T. Shibauchi, Y. Matsuda, and T. Terashima, *Phys. Rev. B* **81**, 020503(R) (2010).
- [22] H.-J. Grafe, D. Paar, G. Lang, N. J. Curro, G. Behr, J. Werner, J. Hamann-Borrero, C. Hess, N. Leps, R. Klingeler, and B. Büchner, *Phys. Rev. Lett.* **101**, 047003 (2008).
- [23] F. L. Ning, K. Ahilan, T. Imai, A. S. Sefat, M. A. McGuire, B. C. Sales, D. Mandrus, P. Cheng, B. Shen, and H.-H. Wen, *Phys. Rev. Lett.* **104**, 037001 (2010).
- [24] T. Dey, P. Khuntia, A.V. Mahajan, S. Sharma, and A. Bharathi, *J. Phys.: Condens. Matter* **23**, 475701 (2011).
- [25] Z. Guguchia, J. Roos, A. Shengelaya, S. Katrych, Z. Bukowski, S. Weyeneth, F. Muranyi, S. Strassle, A. Maisuradze, J. Karpinski, and H. Keller, *Phys. Rev. B* **83**, 144516 (2011).
- [26] R. Sarkar, R. Nath, P. Khuntia, H. S. Jeevan, P. Gegenwart, and M. Baenitz, *J. Phys.: Condens. Matter* **24**, 045702 (2012).
- [27] S. W. Zhang, L. Ma, Y. D. Hou, J. Zhang, T. L. Xia, G. F. Chen, J. P. Hu, G. M. Luke, and W. Yu, *Phys. Rev. B* **81**, 012503 (2010).
- [28] H. Fukazawa, T. Yamazaki, K. Kondo, Y. Yamada, T. Saito, Y. Kohori, N. Takeshita, P. M. Shirage, K. Kihou, K. Miyazawa, H. Kito, A. Iyo, and H. Eisaki, *Physica C* **470**, S464 (2010).
- [29] T. Moriya, *Prog. Theor. Phys.* **16**, 23 (1956); T. Moriya, *J. Phys. Soc. Japan* **18**, 516 (1963); A. V. Mahajan, R. Sala, E. Lee, F. Borsa, S. Kondo, and D. C. Johnston, *Phys. Rev. B* **57**, 8890 (1998).
- [30] E. R. Andrew and D. P. Tunstall, *Proc. Phys. Soc.* **78**, 1 (1961).
- [31] A. Suter, M. Mali, J. Roos, and D. Brinkmann, *J. Phys.: Condens. Matter* **10**, 5977 (1998).
- [32] W. W. Simmons, W. J. O'Sullivan, and W. A. Robinson, *Phys. Rev.* **127**, 1168 (1962).